ELSEVIER
SCIENCE DIRECT
PHYSICS LETTERS B
Physics Letters B 614 (2005) 27–36
www.elsevier.com/locate/physletb

Spectra of prompt electrons from decays of B^+ and B^0 mesons and ratio of inclusive semielectronic branching fractions

Belle Collaboration

T. Okabe [t], K. Abe [h], K. Abe [an], I. Adachi [h], H. Aihara [ap], M. Akatsu [t], Y. Asano [at], T. Aushev [k], A.M. Bakich [ak], Y. Ban [ae], S. Banerjee [al], A. Bay [p], I. Bedny [a], U. Bitenc [l], I. Bizjak [l], S. Blyth [x], A. Bondar [a], A. Bozek [y], M. Bračko [h,r,l], J. Brodzicka [y], T.E. Browder [g], Y. Chao [x], A. Chen [v], K.-F. Chen [x], W.T. Chen [v], B.G. Cheon [c], R. Chistov [k], S.-K. Choi [f], Y. Choi [aj], Y.K. Choi [aj], A. Chuvikov [af], S. Cole [ak], J. Dalseno [s], M. Danilov [k], M. Dash [au], A. Drutskoy [d], S. Eidelman [a], V. Eiges [k], Y. Enari [t], S. Fratina [l], N. Gabyshev [a], A. Garmash [af], T. Gershon [h], A. Go [v], G. Gokhroo [al], B. Golob [q,l], J. Haba [h], T. Hara [ac], K. Hayasaka [t], H. Hayashii [u], M. Hazumi [h], T. Higuchi [ap], L. Hinz [p], T. Hokuue [t], Y. Hoshi [an], S. Hou [v], W.-S. Hou [x], T. Iijima [t], A. Imoto [u], K. Inami [t], A. Ishikawa [h], R. Itoh [h], Y. Iwasaki [h], J.H. Kang [av], J.S. Kang [n], P. Kapusta [y], N. Katayama [h], H. Kawai [b], T. Kawasaki [aa], H. Kichimi [h], H.J. Kim [o], J.H. Kim [aj], S.M. Kim [aj], K. Kinoshita [d], P. Koppenburg [h], S. Korpar [r,l], P. Krokovny [a], C.C. Kuo [v], Y.-J. Kwon [av], J.S. Lange [e], S.E. Lee [ai], S.H. Lee [ai], T. Lesiak [y], J. Li [ah], A. Limosani [s], S.-W. Lin [x], D. Liventsev [k], J. MacNaughton [j], G. Majumder [al], F. Mandl [j], T. Matsumoto [ar], A. Matyja [y], W. Mitaroff [j], H. Miyake [ac], H. Miyata [aa], R. Mizuk [k], D. Mohapatra [au], G.R. Moloney [s], T. Nagamine [ao], Y. Nagasaka [i], E. Nakano [ab], M. Nakao [h], Z. Natkaniec [y], S. Nishida [h], O. Nitoh [as], T. Nozaki [h], S. Ogawa [am], T. Ohshima [t], S. Okuno [m], S.L. Olsen [g], W. Ostrowicz [y], H. Palka [y], C.W. Park [aj], H. Park [o], K.S. Park [aj], N. Parslow [ak], R. Pestotnik [l], L.E. Piilonen [au], M. Rozanska [y], H. Sagawa [h], Y. Sakai [h], T.R. Sarangi [h], T. Schietinger [p], O. Schneider [p], J. Schümann [x], C. Schwanda [j], S. Semenov [k], R. Seuster [g], M.E. Sevior [s], H. Shibuya [am], J.B. Singh [ad], A. Somov [d], N. Soni [ad], R. Stamen [h], S. Stanič [at,1], M. Starič [l], A. Sugiyama [ag], K. Sumisawa [ac], T. Sumiyoshi [ar], S. Suzuki [ag], S.Y. Suzuki [h], O. Tajima [h], F. Takasaki [h], N. Tamura [aa], M. Tanaka [h], Y. Teramoto [ab], X.C. Tian [ae], T. Tsukamoto [h], S. Uehara [h], K. Ueno [x], T. Uglov [k], S. Uno [h], G. Varner [g], K.E. Varvell [ak], C.C. Wang [x], C.H. Wang [w], M.-Z. Wang [x], M. Watanabe [aa], Y. Watanabe [aq],

doi:10.1016/j.physletb.2005.03.060

B.D. Yabsley [au], A. Yamaguchi [ao], Y. Yamashita [z], M. Yamauchi [h], Heyoung Yang [ai], J. Ying [ae], Y. Yusa [ao], J. Zhang [h], L.M. Zhang [ah], Z.P. Zhang [ah], V. Zhilich [a], D. Žontar [q,l]

[a] *Budker Institute of Nuclear Physics, Novosibirsk, Russia*
[b] *Chiba University, Chiba, Japan*
[c] *Chonnam National University, Kwangju, South Korea*
[d] *University of Cincinnati, Cincinnati, OH, USA*
[e] *University of Frankfurt, Frankfurt, Germany*
[f] *Gyeongsang National University, Chinju, South Korea*
[g] *University of Hawaii, Honolulu, HI, USA*
[h] *High Energy Accelerator Research Organization (KEK), Tsukuba, Japan*
[i] *Hiroshima Institute of Technology, Hiroshima, Japan*
[j] *Institute of High Energy Physics, Vienna, Austria*
[k] *Institute for Theoretical and Experimental Physics, Moscow, Russia*
[l] *J. Stefan Institute, Ljubljana, Slovenia*
[m] *Kanagawa University, Yokohama, Japan*
[n] *Korea University, Seoul, South Korea*
[o] *Kyungpook National University, Taegu, South Korea*
[p] *Swiss Federal Institute of Technology of Lausanne, EPFL, Lausanne*
[q] *University of Ljubljana, Ljubljana, Slovenia*
[r] *University of Maribor, Maribor, Slovenia*
[s] *University of Melbourne, Victoria, Australia*
[t] *Nagoya University, Nagoya, Japan*
[u] *Nara Women's University, Nara, Japan*
[v] *National Central University, Chung-li, Taiwan*
[w] *National United University, Miao Li, Taiwan*
[x] *Department of Physics, National Taiwan University, Taipei, Taiwan*
[y] *H. Niewodniczanski Institute of Nuclear Physics, Krakow, Poland*
[z] *Nihon Dental College, Niigata, Japan*
[aa] *Niigata University, Niigata, Japan*
[ab] *Osaka City University, Osaka, Japan*
[ac] *Osaka University, Osaka, Japan*
[ad] *Panjab University, Chandigarh, India*
[ae] *Peking University, Beijing, PR China*
[af] *Princeton University, Princeton, NJ, USA*
[ag] *Saga University, Saga, Japan*
[ah] *University of Science and Technology of China, Hefei, PR China*
[ai] *Seoul National University, Seoul, South Korea*
[aj] *Sungkyunkwan University, Suwon, South Korea*
[ak] *University of Sydney, Sydney, NSW, Australia*
[al] *Tata Institute of Fundamental Research, Bombay, India*
[am] *Toho University, Funabashi, Japan*
[an] *Tohoku Gakuin University, Tagajo, Japan*
[ao] *Tohoku University, Sendai, Japan*
[ap] *Department of Physics, University of Tokyo, Tokyo, Japan*
[aq] *Tokyo Institute of Technology, Tokyo, Japan*
[ar] *Tokyo Metropolitan University, Tokyo, Japan*
[as] *Tokyo University of Agriculture and Technology, Tokyo, Japan*
[at] *University of Tsukuba, Tsukuba, Japan*
[au] *Virginia Polytechnic Institute and State University, Blacksburg, VA, USA*
[av] *Yonsei University, Seoul, South Korea*

Received 22 November 2004; accepted 23 March 2005

Available online 1 April 2005

Editor: M. Doser

Abstract

We present spectra of prompt electrons from decays of neutral and charged B mesons. The results are based on 140 fb^{-1} of data collected by the Belle detector on the $\Upsilon(4S)$ resonance at the KEKB e^+e^- asymmetric collider. We tag $\Upsilon(4S) \to B\bar{B}$ events by reconstructing a B meson in one of several hadronic decay modes; the semileptonic decay of the other B meson is inferred from the presence of an identified electron. We obtain for charged and neutral B mesons the partial rates of semileptonic decay, to electrons with momentum greater than 0.6 GeV/c in the B rest frame, and their ratio $b_+/b_0 = 1.08 \pm 0.05 \pm 0.02$, where the first and second errors are statistical and systematic, respectively.

PACS: 13.20.He

Keywords: Semileptonic; B decay; Inclusive

1. Introduction

The inclusive semileptonic B meson decay branching fraction $\mathcal{B}(B \to X\ell\nu)$ is a fundamental quantity that is required to fully understand B meson decays. The decay is believed to be dominated by a spectator process, where the b quark is coupled to a c or u quark and a virtual W boson, while the accompanying quark in the meson, the so-called spectator, plays no direct role. Therefore, the theoretical treatment is relatively simple, and the semileptonic width Γ_{SL} can be readily predicted. However, it has long been a puzzle that while theoretical calculations predict values of $\mathcal{B}(B \to X\ell\nu)$ higher than 12% [1], most measurements have been consistently lower, at 10–11% [2]. The discrepancy may be attributed to the uncertainty in predicting the hadronic decay width Γ_{had}, where contributions from non-spectator processes are significant. The non-spectator contribution depends on the flavor of the accompanying quark, while this is not the case for Γ_{SL}. Therefore, it may result in unequal $\mathcal{B}(B \to X\ell\nu)$ values for neutral and charged B mesons, hereafter referred to as b_0 and b_+, respectively. The ratio b_+/b_0 is equal to the B lifetime ratio τ_+/τ_0 assuming equality in Γ_{SL}. The B lifetime ratio is measured well [2]. However, only a few measurements have addressed b_+ and b_0 separately, and the uncertainties have been large due to low efficiencies for tagging neutral and charged events [3]. The deviations from unity for both the lifetime ratio and the b_+/b_0 ratio are predicted to be of order 10% [4].

Furthermore, measurement of $\mathcal{B}(B \to X\ell\nu)$ combined with the lifetime is one of the favored methods to determine the Cabibbo–Kobayashi–Maskawa matrix element $|V_{cb}|$ [5]. Heavy-quark-expansions (HQEs) [6] have become a useful tool to calculate the correction due to strong interaction effects. There have been some attempts to improve the determination of $|V_{cb}|$, by fitting the perturbative and non-perturbative parameters in HQEs to the data of the hadronic invariant mass (M_X) and the lepton energy (E_ℓ) moments in the B semileptonic decay [7]. Recently, the BaBar Collaboration performed a fit to the partial $B \to X_c e\nu$ branching fraction and the M_X and E_ℓ moments, with varied cutoffs on the lepton energy, to extract $|V_{cb}|$ and the total $B \to X_c e\nu$ branching fraction as well as the HQE parameters [8] on a consistent basis.

In this Letter we report measurements of b_0 and b_+ in the electronic channel with an electron momentum requirement $p^* \geqslant 0.6$ GeV/c, as measured in the rest frame of the B meson. These measurements are based on data collected by the Belle detector [9] at the KEKB asymmetric e^+e^- collider [10], which provides copious production of $B\bar{B}$ meson pairs on the $\Upsilon(4S)$ resonance. In this analysis, one B meson is fully reconstructed in one of several hadronic decay modes to determine its charge, fla-

E-mail address: okabe@hepl.phys.nagoya-u.ac.jp (T. Okabe).

[1] On leave from Nova Gorica Polytechnic, Nova Gorica, Slovenia.

vor, and momentum, and is referred to as the tag side B (B_{tag}) in the event. The semileptonic decay of the other B meson, referred to as the spectrum side B (B_{spec}), is then measured in its rest frame, determined from B_{tag}, without smearing due to the B motion. Prompt semileptonic decays ($b \to xe\nu$) can be separated from secondary decays ($b \to c \to ye\nu$), based on the correlation between the B_{tag} flavor and the electron charge. To exploit the advantages of this method requires a large sample of $B\bar{B}$ events because the full reconstruction efficiency is rather low, typically of the order of 0.1%. Our high integrated luminosity enables us to perform this measurement with higher accuracy than previously achieved.

2. Data set and Belle detector

The results presented in this Letter are based on a 140 fb^{-1} data sample accumulated on the $\Upsilon(4S)$ resonance, which contains $152.0 \times 10^6 B\bar{B}$ pairs. The center-of-mass energy is $\sqrt{s} \simeq 10.58$ GeV. An additional 15 fb^{-1} data sample taken at a center-of-mass energy 60 MeV below the $\Upsilon(4S)$ resonance is used to evaluate background from the $e^+e^- \to q\bar{q}$ ($q = u, d, s, c$) process. A detailed Monte Carlo (MC) simulation, which fully describes the detector geometry and response and is based on GEANT [11], is applied to study backgrounds in the B_{tag} reconstruction, backgrounds in the signal electron detection, and corrections to the signal selection efficiency due to the tagging. In the MC simulation, generic $B\bar{B}$ decays are simulated using the QQ98 generator [12].

The Belle detector is a large-solid-angle magnetic spectrometer that consists of a three-layer silicon vertex detector (SVD), a 50-layer central drift chamber (CDC), an array of aerogel threshold Čerenkov counters (ACC), a barrel-like arrangement of time-of-flight scintillation counters (TOF), and an electromagnetic calorimeter comprised of CsI(Tl) crystals (ECL) located inside a superconducting solenoid coil that provides a 1.5 T magnetic field. An iron flux-return located outside of the coil is instrumented to detect K_L^0 mesons and to identify muons (KLM). The detector is described in detail elsewhere [9].

3. Fully reconstructed tagging

Neutral B_{tag} candidates are reconstructed in the decay modes $B^0 \to D^{*-}\pi^+$, $D^{*-}\rho^+$, $D^{*-}a_1^+$ and $B^0 \to D^-\pi^+$, $D^-\rho^+$, $D^-a_1^+$. Charged B_{tag} candidates are reconstructed in the decay modes $B^+ \to \bar{D}^{*0}\pi^+$, $\bar{D}^{*0}\rho^+$, $\bar{D}^{*0}a_1^+$ and $B^+ \to \bar{D}^0\pi^+$. The decay modes $B^+ \to \bar{D}^0\rho^+$ and $\bar{D}^0a_1^+$ are not used here because of poor purity due to large combinatorial background. Inclusion of the charge conjugate decays is implied throughout this Letter.

To suppress the non-$b\bar{b}$ background processes from QED, $e^+e^- \to \tau^+\tau^-$, and beam-gas events, we select hadronic events based on the charged track multiplicity and total visible energy. The selection procedure is described in detail elsewhere [13].

Charged particle tracks are reconstructed from hits in the SVD and CDC. They are required to satisfy track quality based on their impact parameters relative to the measured profile of the interaction point (IP profile) of the two beams, and good measurements in the SVD in the direction of the beam (z). Charged kaons are identified by combining information on energy deposit (dE/dx) in the CDC, Čerenkov light yields in the ACC and time-of-flight measured by the TOF system. For the nominal requirement, the kaon identification efficiency is approximately 88% and the rate for misidentification of pions as kaons is about 8%. Hadron tracks that are not identified as kaons are treated as pions. Tracks satisfying the lepton identification criteria are removed from consideration.

Candidate π^0 mesons are reconstructed using γ pairs with an invariant mass within ± 30 MeV/c^2 of the nominal π^0 mass. Each γ is required to have a minimum energy deposit of: $E_\gamma \geqslant 50$ MeV in the barrel region of the ECL, defined as $32° < \theta_\gamma < 129°$; $E_\gamma \geqslant 100$ MeV in the forward endcap region, defined as $12° < \theta_\gamma < 31°$; $E_\gamma \geqslant 150$ MeV in the backward endcap region, defined as $131° < \theta_\gamma < 155°$, where θ_γ denotes the polar angle of the γ with respect to the direction opposite to the positron beam. K_S^0 mesons are reconstructed using pairs of charged tracks that have a well reconstructed vertex that is displaced from the IP and an invariant mass within ± 7.6 MeV/c^2 of the known K_S^0 mass. ρ^+ and ρ^0 candidates are reconstructed in the $\pi^+\pi^0$ and $\pi^+\pi^-$ decay modes by requiring their invariant masses to be within ±150 MeV$/c^2$ of the nominal ρ mass. The ρ^+ candidates are required to satisfy $\cos\theta_\rho \geqslant -0.9$, where θ_ρ is the helicity angle, defined as the angle between an axis anti-parallel to the B flight direction and the π^+ flight direction in the ρ rest frame. a_1^+ candidates are formed from combinations of ρ^0 and π^+ candidates by requiring that the three tracks form a good vertex and have an invariant mass between 0.73 GeV$/c^2$ and 1.73 GeV$/c^2$.

$\bar{D}^0$ candidates are reconstructed in the four decay modes $\bar{D}^0 \to K^+\pi^-$, $K^+\pi^-\pi^0$, $K^+\pi^+\pi^-\pi^-$ and $K_S^0\pi^+\pi^-$. D^- candidates are reconstructed in the decay mode $D^- \to K^+\pi^-\pi^-$. The D^0 (D^-) candidates are required to have an invariant mass within $\pm30(12)$ MeV$/c^2$ of the nominal D^0 (D^-) mass. $\bar{D}^*$ mesons are reconstructed by pairing $\bar{D}^0$ candidates with pions, $D^{*-} \to \bar{D}^0\pi^-$ and $\bar{D}^{*0} \to \bar{D}^0\pi^0$. The $\bar{D}\pi$ pairs are required to have a mass difference $\Delta m = m_{\bar{D}\pi} - m_{\bar{D}}$ within 0.142 GeV$/c^2 < \Delta m <$ 0.149 GeV$/c^2$ for D^{*+}, and 0.140 GeV$/c^2 < \Delta m <$ 0.145 GeV$/c^2$ for D^{*0}. All D^0 candidates are used for B reconstruction, regardless of whether or not the D^0 candidate is used to reconstruct a D^* meson.

The selection of B candidates is based on the beam-constrained mass, $M_{bc} = \sqrt{E_{beam}^2 - p_B^2}$, and the energy difference, $\Delta E = E_B - E_{beam}$, where $E_{beam} \equiv \sqrt{s}/2 \simeq 5.290$ GeV, and p_B and E_B are the momentum and energy of the reconstructed B in the $\Upsilon(4S)$ rest frame, respectively. The background from jet-like $e^+e^- \to q\bar{q}$ processes is suppressed by event topology based on the normalized second Fox–Wolfram moment (R_2) [14] and the angle between the thrust axis of the B candidate and that of the remaining tracks in an event ($\cos\theta_{th}$). Requirements on R_2 and $\cos\theta_{th}$, as well as the K/π selection, are tuned to suppress the background and depend on the B_{tag} decay mode. We select B_{tag} candidates in a signal region defined as 5.27 GeV$/c^2 \leqslant M_{bc} \leqslant 5.29$ GeV$/c^2$ and $|\Delta E| \leqslant 0.05$ GeV.

Fig. 1 shows the distribution in M_{bc} for the neutral and charged B candidates in the ΔE signal region. The M_{bc} signal regions, indicated by arrows in Fig. 1, contain 36974 and 36418 B^0 and B^+ candidates, respectively. The contribution from the $q\bar{q}$ process is estimated by scaling the off-resonance data by the luminosity ratio with a small correction due to the energy dependence of the cross section and found to be 2584 ± 154 (2630 ± 156) for B^0 (B^+) candidates. The B candidates remaining after the $q\bar{q}$ background subtraction contain combinatorial background from B decays, where some particles are exchanged between the tag and the spectrum sides (cross-talk). We estimate the contribution from such combinatorial background to be 3221 ± 372 (667 ± 162) for B^0 (B^+) candidates, by scaling the M_{bc} distribution in the high ΔE sideband (0.07 GeV $\leqslant \Delta E \leqslant$ 0.30 GeV) with normalization to the yields in the M_{bc} sideband ($M_{bc} \leqslant 5.26$ GeV$/c^2$) after the $q\bar{q}$ background subtraction. Note that we do not apply best B_{tag} candidate selection for events having multiple candidates, in order to avoid distorting the ΔE distribution. The remaining 31169 ± 446 (33121 ± 295) B^0 (B^+) candi-

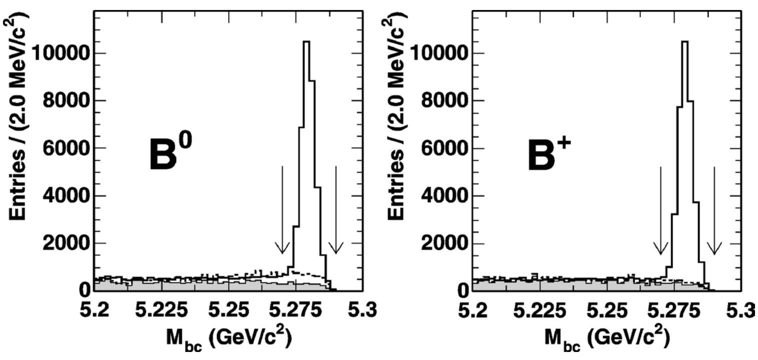

Fig. 1. Beam-constrained mass (M_{bc}) distributions for B^0 and B^+ candidates with a $|\Delta E| \leqslant 0.05$ GeV requirement. The solid histogram corresponds to the on-resonance data. The hatched histogram is for the off-resonance data scaled by luminosity. The dashed histogram indicates the contribution from the combinatorial background estimated by scaling the ΔE sideband (0.07 GeV $\leqslant \Delta E \leqslant$ 0.30 GeV). The arrows indicate the M_{bc} signal region.

dates, denoted as $N_{\text{tag}}(B^0)$ ($N_{\text{tag}}(B^+)$), are from $B\bar{B}$ events, and are used to normalize the lepton yield to obtain the semileptonic branching fraction. These B_{tag} candidates may include a small fraction with incorrectly assigned B charge and/or flavor due to particles that are not detected. The rate of such misassignment is found to be 0.6% (1.9%) for events with (without) electrons on the spectrum side, according to the MC simulation, and its effect on the determination of b_+ and b_0 is found to be less than 0.1%. In order to obtain the electron spectra, presented later, we apply the same background subtraction to determine the electron yield for tagged events in each electron momentum bin.

4. Electron selection and background subtraction

For events passing our B_{tag} selection, we search for electrons from semileptonic decays of B_{spec}. The electron momentum (p^*) is measured in the B rest frame, which is found using the B_{tag} momentum. Electrons are divided into two categories, based on the correlation between the electron charge (q_e) and B_{tag} flavor (Q_{tag}). With the assignment $Q_{\text{tag}} = +1$ (-1) for $\bar{B}^0$ and B^- (B^0 and B^+), electrons having $q_e \times Q_{\text{tag}} = +1$ (-1) are referred to as “right (wrong) sign” electrons.

Electron identification is based on a combination of dE/dx in the CDC, the response of the ACC, shower shape in the ECL and the ratio of energy deposit in the ECL to the momentum measured by the tracking system [15]. The electron identification efficiency depends on the track momentum. Based on the MC simulation, the efficiencies are estimated to be about 90% in the momentum region above 1.2 GeV/c in the B rest frame, where electrons from the prompt B decays dominate. The rate of pions (kaons) to be misidentified as electrons is measured using reconstructed $K_S^0 \to \pi^+\pi^-$ ($D^{*+} \to D^0\pi^+$ ($D^0 \to K^-\pi^+$)) and found to be less than 0.2% for electrons in the same momentum region.

For the determination of semileptonic branching fractions we use electron candidates with $p^* \geqslant 0.6$ GeV/c. We demand that electrons be detected in the barrel region of the associated detector system and with sufficient transverse energy for a good measurement; we make requirements on the laboratory transverse momenta with respect to the direction opposite to the positron beam, $p_t \geqslant 0.6$ GeV/c, and on the laboratory polar angle, $35° \leqslant \theta \leqslant 125°$. Radiative energy loss by electrons is corrected for by adding back energy found in ECL clusters within 3 degrees of the reconstructed momentum direction. Backgrounds from J/ψ decays, photon conversions in the detector and π^0 Dalitz decays are suppressed by imposing veto conditions; we calculate invariant masses for each electron candidate when combined with opposite charge electrons (m_{ee}) and with additional photons ($m_{ee\gamma}$), and reject the electron if m_{ee} lies within ± 49 MeV/c^2 of the nominal J/ψ mass, m_{ee} is less

Table 1
Summary of electron yields and estimated backgrounds

	B^0 candidate		B^+ candidate	
	e: right-sign	e: wrong-sign	e: right-sign	e: wrong-sign
On-resonance data	2007.0 ± 44.8	967.0 ± 31.1	2520.0 ± 50.2	450.0 ± 21.2
Scaled off resonance	9.2 ± 9.2	0.0 ± 9.2	9.2 ± 9.2	0.0 ± 9.2
Estimated combinatorial	78.6 ± 10.5	33.9 ± 5.5	31.9 ± 6.9	12.7 ± 3.3
Estimated background	130.7 ± 1.3	73.9 ± 1.1	154.3 ± 1.0	46.6 ± 0.5
From J/ψ	2.8 ± 0.1	2.9 ± 0.1	3.0 ± 0.1	3.0 ± 0.1
From Dalitz or conv.	25.7 ± 0.4	25.9 ± 0.4	27.7 ± 0.4	27.5 ± 0.4
From τ	42.7 ± 0.5	10.1 ± 0.2	52.6 ± 0.6	0.8 ± 0.1
From upper vertex	50.9 ± 0.5	27.3 ± 0.4	60.5 ± 0.6	9.5 ± 0.2
Hadron fakes	8.6 ± 1.0	7.7 ± 0.9	10.5 ± 0.3	5.8 ± 0.2
Bkg. subtracted	1788.5 ± 47.4	859.2 ± 34.0	2324.4 ± 51.4	390.7 ± 23.3
After mixing corr.	2063.7 ± 62.3	584.0 ± 46.3		
After eff. corr.	3298.6 ± 104.2	1067.3 ± 80.8	3736.7 ± 84.0	713.5 ± 42.6

than 100 MeV/c^2 or $m_{ee\gamma}$ is within ±32 MeV/c^2 of the nominal π^0 mass.

The obtained electron spectra include events from several background processes. Table 1 summarizes the number of detected electrons and the contributions from each background source.

Backgrounds from J/ψ decays, photon conversion and π^0 Dalitz decays are small after the veto. The remaining backgrounds, where one of the pair has escaped detection, are estimated by the MC simulation. The background from these processes amounts to 2.0% of the yield in the signal region. The uncertainties are evaluated from the error on each rate.

Contributions from secondary electrons from B decays are modeled by the MC simulation based on Ref. [12] and branching fractions quoted in Ref. [2]. These include leptons from τ decays in processes such as $B \to X\tau^+\nu$ and $B \to D_s X$ followed by $D_s \to \tau^+\nu$. The uncertainty of their contribution is estimated based on $\mathcal{B}(b \to \tau\nu + \text{anything}) = (2.48 \pm 0.26)\%$ in Ref. [2]. Another major source of secondary electrons is the $W^+ \to c\bar{s}(c\bar{d})$ processes ("upper vertex" charm) such as $B \to D_s X$, $D_s \to Y\ell^+\nu$ and $B \to D^{(*)}D^{(*)}K^{(*)}$, $D \to Y\ell^+\nu$ via $\bar{b} \to \bar{c}c\bar{s}$ and a small contribution from $B \to D^{(*)}D^{(*)}$. The uncertainty of their contribution is estimated based on $\mathcal{B}(\bar{b} \to \bar{c}c\bar{s}) = (22 \pm 4)\%$ in Ref. [2]. The backgrounds from these processes account for 4.3% of the yield in the signal region. The uncertainties are evaluated from the errors on the associated branching fractions.

Contributions from misidentified hadrons are estimated by multiplying the measured fake rates by the number of additional hadron tracks in events containing selected B_{tag}. Here, the hadrons are obtained by imposing a lepton identification veto on charged tracks. Misidentified hadrons are distributed mainly in the momentum region below 1.5 GeV/c, and amount to 0.4% (1.0%) over the whole momentum range of the right (wrong) sign spectra.

5. Semileptonic decay spectra

The spectra after the above background subtraction contain electrons from prompt semileptonic B decays and from secondary semileptonic charm decays ("lower vertex" charm). After background subtraction, the number of right (wrong) sign electrons is 1789 ± 47 (859 ± 34) for events tagged with B^0, and 2324 ± 51 (391 ± 23) for those tagged with B^+. For events tagged with a B^+, electrons with the right and wrong signs correspond to those from prompt B and secondary charm decays, respectively. For events tagged with a B^0, the effect of B^0–$\bar{B}^0$ mixing is taken into account, by solving the following equations for N_{p} and N_{s}, the number of electrons from prompt and secondary semileptonic decays, respectively:

$$N_{\text{right}} = N_{\text{p}}(1 - \chi_d) + N_{\text{s}}\chi_d,$$
$$N_{\text{wrong}} = N_{\text{p}}\chi_d + N_{\text{s}}(1 - \chi_d),$$

where N_{right} and N_{wrong} are the numbers of right- and wrong-sign electrons and $\chi_d = 0.186 \pm 0.004$ [2] is the B^0–$\bar{B}^0$ mixing probability.

The electron detection efficiency is corrected for detector acceptance, tracking and electron selection efficiencies, where the correction is evaluated with the MC simulation. We also take into account a correlation due to the difference in the event tagging efficiency between events where the B_{spec} decays semileptonically and those where it decays hadronically. This effect is referred to hereafter as "tag bias". In the MC simulation, it is found that the difference depends on track multiplicity in the event, which alters the detection efficiency of charged, π^0 and K_S^0 particles used for the B_{tag} reconstruction. The tag bias effect is estimated from the change of semileptonic decay fraction in the tagged sample using the generator information in the MC simulation, which is 8% (6%) for B^0 (B^+). Fig. 2 shows the p^* spectra from the prompt B and the secondary semileptonic decays obtained separately for B^0 and B^+. The differential branching fractions $d\mathcal{B}/dp$ are obtained from the number of electrons, normalized by $N_{\text{tag}}(B^0)$ or $N_{\text{tag}}(B^+)$. Table 2 shows obtained differential branching fraction for each bin. Both in Fig. 2 and Table 2, the errors are statistical only. The analysis of systematic uncertainties presented in detail in Section 6 shows that they are momentum independent and the common systematic error of 3.4% and 3.6% can be ascribed to all the bins for B^0 and B^+, respectively.

The partial branching fractions for the electron channel, integrated over the momentum region above 0.6 GeV/c, are $b_0(p^* \geqslant 0.6\ \text{GeV}/c) = (9.83 \pm 0.34)\%$ and $b_+(p^* \geqslant 0.6\ \text{GeV}/c) = (10.62 \pm 0.25)\%$ for B^0 and B^+, respectively. Their average and ra-

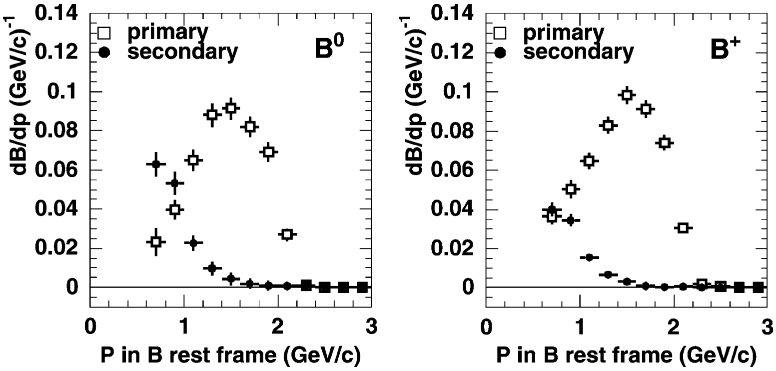

Fig. 2. Momentum spectra in the B meson rest frame of electrons from prompt semileptonic B decay (open squares) and secondary semileptonic charm decay (closed circles) for B^0 and B^+ tagged events. The vertical scale shows the differential branching fraction ($d\mathcal{B}/dp$).

Table 2
Differential branching fractions of B^0 and B^+ for each bin. The last column shows their ratio. The errors are statistical only. The common systematic error of 3.4%, 3.6% and 1.9% can be ascribed to all the bins for B^0, B^+ and B^+/B^0, respectively

$d\mathcal{B}/dp$ $(\text{GeV}/c)^{-1}$			
p (GeV/c)	B^0	B^+	B^+/B^0
0.6–0.8	0.0234 ± 0.0071	0.0362 ± 0.0040	1.547 ± 0.502
0.8–1.0	0.0401 ± 0.0053	0.0503 ± 0.0047	1.253 ± 0.203
1.0–1.2	0.0656 ± 0.0056	0.0648 ± 0.0042	0.987 ± 0.106
1.2–1.4	0.0889 ± 0.0061	0.0831 ± 0.0045	0.934 ± 0.082
1.4–1.6	0.0925 ± 0.0058	0.0985 ± 0.0048	1.065 ± 0.085
1.6–1.8	0.0829 ± 0.0055	0.0913 ± 0.0046	1.101 ± 0.091
1.8–2.0	0.0700 ± 0.0050	0.0742 ± 0.0041	1.060 ± 0.096
2.0–2.2	0.0271 ± 0.0031	0.0304 ± 0.0026	1.121 ± 0.160
2.2–2.4	0.0010 ± 0.0007	0.0019 ± 0.0007	1.892 ± 1.408
2.4–2.6	0.0001 ± 0.0002	0.0005 ± 0.0003	3.912 ± 5.849

tio are found to be $b(p^* \geqslant 0.6\ \text{GeV}/c) = (10.34 \pm 0.20)\%$, and $b_+/b_0(p^* \geqslant 0.6\ \text{GeV}/c) = 1.08 \pm 0.05$.

6. Systematic error

The systematic uncertainties on the partial semileptonic branching fractions are evaluated separately for b_0 and b_+, and are summarized in Table 3.

The uncertainty in N_{tag} is associated mainly with the procedure for the combinatorial background subtraction described earlier. After applying the same procedure on the simulated data and comparing the number of obtained tagged candidates with the true number, the systematic uncertainty due to N_{tag} determination is estimated to be 1.0–1.9%.

The uncertainty due to the tag bias correction is estimated to be 1.3% from the uncertainties of the charged particle and photon multiplicity dependence in the B_{tag} reconstruction. We find multiplicity difference between data and the simulation to be about 0.1 for charged particles and 0.2 for photons. These differences propagate to the reconstruction efficiencies of charged particles, π^0 and K_S^0, and hence the B_{tag} which is reconstructed based on 8.1 charged particles, $2.7\pi^0$ and $1.1K_S^0$ per event on average. We add another 1.8% (1.6%) uncertainty due to the statistics in the MC simulation to determine the tag bias correction factor for B^0 (B^+).

The uncertainty on the tracking efficiency is determined based on a study using $D^{*+} \to D^0(\to K_S^0\pi^+\pi^-)\pi^+$ decays. In this study, the yield of fully reconstructed D^* mesons is to be compared to that using partial reconstruction, where one pion from K_S^0 is not used. A $\pm 1.0\%$ uncertainty is assigned for the tracking efficiency by taking the difference of the yield ratio between the experimental data and the MC simulation.

The uncertainty on the electron identification efficiency is one of the largest sources of systematic error. It is estimated to be $\pm 2.1\%$ from the difference between the efficiency determined from the MC simulation and that based on a sample of simulated tracks embedded in beam data. The uncertainty on the fake electron rate is studied by comparing the fake rates measured with $K_S^0 \to \pi^+\pi^-$ decays in real data and

Table 3
Contributions to the systematic error

Source	$\Delta b_0/b_0$ (%)	$\Delta b_+/b_+$ (%)	$\Delta \frac{b_+}{b_0} / \frac{b_+}{b_0}$ (%)
N_{tag}	± 1.0	± 1.9	± 1.9
Tag-bias	± 2.2	± 2.1	–
Tracking	± 1.0	± 1.0	–
PID efficiency	± 2.1	± 2.1	< 0.1
Hadron fakes	± 0.1	± 0.1	< 0.1
e from J/ψ	< 0.1	< 0.1	< 0.1
e from conversion	< 0.1	< 0.1	< 0.1
e from τ	± 0.3	± 0.3	< 0.1
e from upper vertex	± 0.6	± 0.5	< 0.1
Mixing	± 0.4	–	± 0.4
Continuum subtraction	± 0.1	± 0.1	± 0.1
Total	± 3.4	± 3.6	± 1.9

in the MC simulation. The uncertainty on b_0 and b_+ is estimated to be $\pm 0.1\%$.

The uncertainties on the background subtractions from J/ψ decays, converted electrons, τ decays, and the "upper vertex" processes are evaluated from the error on each rate, as described above. The uncertainty in b_0 and b_+ for the "upper vertex" processes is (0.5–0.6)%.

The uncertainty from the mixing probability χ_d is determined based on its quoted error in Ref. [2], and contributes $\pm 0.4\%$ to the systematic error on b_0.

The uncertainty in the continuum subtraction is attributed to the normalization between on- and off-resonance data, and is estimated to be $\pm 0.1\%$ based on the error of the relative luminosity measurement.

The overall systematic errors are evaluated by adding these errors in quadrature. The systematic error on the ratio b_+/b_0 is small because several sources of systematic error cancel in the ratio. The remaining sources of systematic error are mainly $N(B_{\text{tag}})$ estimation (1.9%) and mixing (0.4%). The overall systematic errors on the partial branching fractions are 3.6% for b_+, 3.4% for b_0 and 1.9% for b_+/b_0.

7. Results and summary

Including the above systematic errors, the partial semileptonic branching fractions are

$$b_0\big(p^* \geqslant 0.6\ \text{GeV}/c\big) = (9.83 \pm 0.34 \pm 0.33)\%,$$
$$b_+\big(p^* \geqslant 0.6\ \text{GeV}/c\big) = (10.62 \pm 0.25 \pm 0.39)\%$$

and their average and ratio are found to be

$$b\big(p^* \geqslant 0.6\ \text{GeV}/c\big) = (10.34 \pm 0.20 \pm 0.36)\%,$$
$$b_+/b_0\big(p^* \geqslant 0.6\ \text{GeV}/c\big) = 1.08 \pm 0.05 \pm 0.02.$$

These average values are calculated with weights determined by the statistical error of each subsample.

The average partial branching fraction b is consistent with our previous measurement [16], with the overall error improved by 15%, and it is also consistent with recent measurements on the $\Upsilon(4S)$ resonance by BaBar and CLEO [17] with the same minimum momentum requirement. Our results are the most precise separate determinations of b_+, b_0 and their ratio b_+/b_0. The observed b_+/b_0 ratio is consistent with the B^+/B^0 lifetime ratio $\tau_+/\tau_0 = 1.086 \pm 0.017$ [2]. Furthermore, as shown in Table 2, the ratio of the differential branching fraction for each momentum bin is consistent with τ_+/τ_0. There is no indication that the naïve expectation of equal Γ_{SL} for charged and neutral B mesons break down in the measured range of electron momentum.

The present analysis method using fully reconstructed tags can be extended to a separate determination of the M_X and E_ℓ moments in the B^+ and B^0 semileptonic decays. The partial branching fractions obtained in the present work can be used as part of a combined fit of HQE parameters to the full set of the moments to determine the total branching fraction as well as $|V_{cb}|$. In contrast to measurements based on samples with B^+/B^0 admixtures, such an approach will help to eliminate the uncertainty in $|V_{cb}|$ due to the production ratio of B^+ and B^0 on the $\Upsilon(4S)$ resonance (f_+/f_0), and will also provide a useful cross check of assumptions behind the HQE theory, such as quark–hadron duality. These extensions to this analysis will be reported in future articles.

Acknowledgements

We thank the KEKB group for the excellent operation of the accelerator, the KEK Cryogenics group for the efficient operation of the solenoid, and the KEK computer group and the National Institute of Informatics for valuable computing and Super-SINET network support. We acknowledge support from:

– The Ministry of Education, Culture, Sports, Science, and Technology of Japan and the Japan Society for the Promotion of Science;
– The Australian Research Council and the Australian Department of Education, Science and Training;
– The National Science Foundation of China under contract No. 10175071;
– The Department of Science and Technology of India;
– The BK21 program of the Ministry of Education of Korea and the CHEP SRC program of the Korea Science and Engineering Foundation;
– The Polish State Committee for Scientific Research under contract No. 2P03B 01324;
– The Ministry of Science and Technology of the Russian Federation;
– The Ministry of Education, Science and Sport of the Republic of Slovenia;
– The Swiss National Science Foundation;
– The National Science Council and the Ministry of Education of Taiwan;
– The US Department of Energy.

References

[1] I. Bigi, B. Blok, M. Shifman, A. Vainshtein, Phys. Lett. B 323 (1994) 408.
[2] S. Eidelman, et al., Particle Data Group, Phys. Lett. B 592 (2004) 1.
[3] CLEO Collaboration, M. Athanas, et al., Phys. Rev. Lett. 73 (1994) 3503;
CLEO Collaboration, M. Artuso, et al., Phys. Lett. B 399 (1997) 321;
U. Langenegger (for BaBar Collaboration), hep-ex/0204001 EPS2001.
[4] G. Bellini, I.I. Bigi, P.J. Dornan, Phys. Rep. 289 (1997) 1.
[5] M. Kobayashi, T. Maskawa, Prog. Theor. Phys. 49 (1973) 652;
N. Cabibbo, Phys. Rev. Lett. 10 (1963) 531.
[6] M. Voloshin, M. Shifman, Sov. J. Nucl. Phys. 41 (1985) 120;
J. Chay, H. Georgi, B. Grinstein, Phys. Lett. B 247 (1990) 399;
I.I. Bigi, N. Uraltsev, Phys. Lett. B 280 (1992) 271.
[7] C.W. Bauer, et al., Phys. Rev. D 67 (2003) 054012;
M. Battaglia, et al., Phys. Lett. B 556 (2003) 41;
C.W. Bauer, et al., hep-ph/0408002.
[8] BaBar Collaboration, B. Aubert, et al., Phys. Rev. Lett. 93 (2004) 011803.
[9] Belle Collaboration, A. Abashian, et al., Nucl. Instrum. Methods A 479 (2002) 117.
[10] S. Kurokawa, E. Kikutani, Nucl. Instrum. Methods A 499 (2003) 1, and other papers included in this volume.
[11] R. Brun, et al., CERN Report No. DD/EE/84-1, 1984.
[12] The QQ B meson event generator was developed by the CLEO Collaboration. See the following URL: http://www.lns.cornell.edu/public/CLEO/soft/QQ.
[13] Belle Collaboration, K. Abe, et al., Phys. Rev. D 64 (2001) 072001.
[14] G.C. Fox, S. Wolfram, Phys. Rev. Lett. 41 (1978) 1581.
[15] K. Hanagaki, et al., Nucl. Instrum. Methods A 485 (2002) 490.
[16] Belle Collaboration, K. Abe, et al., Phys. Lett. B 547 (2002) 181.
[17] BaBar Collaboration, B. Aubert, et al., Phys. Rev. D 69 (2004) 111104(R);
CLEO Collaboration, A.H. Mahmood, et al., Phys. Rev. D 70 (2004) 032003.